

Band or Polaron: The Hole Conduction Mechanism in the p -Type Spinel Rh_2ZnO_4

Arpun R. Nagaraja,^{‡,*} Nicola H. Perry,^{‡,*} Thomas O. Mason,^{‡,†,**} Yang Tang,[§] Matthew Grayson,[§] Tula R. Paudel,[¶] Stephan Lany,[¶] and Alex Zunger[¶]

[‡]Department of Materials Science and Engineering, Northwestern University, Evanston, Illinois 60208

[§]Department of Electrical Engineering and Computer Science, Northwestern University, Evanston, Illinois 60208

[¶]National Renewable Energy Laboratory, Golden, Colorado 80401

Given the emerging role of oxide spinels as hole conductors, we discuss in this article the traditional vs. new methodologies of determining the type of conduction mechanism at play—localized polaronic vs. band-like transport. Applying (i) traditional small polaron analysis to our *in-situ* high temperature four-point conductivity and thermopower measurements, we previously found an activated mobility, which is indicative of the small polaron mechanism. However, (ii) employing the recent developments in correcting density functional methodologies for hole localization, we predict that the self-trapped hole is unstable and that Rh_2ZnO_4 is instead a band conductor with a large effective mass. The hole mobility measured by high-field room temperature Hall effect also suggests band rather than polaron conduction. The apparent contradiction between the conclusion of the traditional procedure (i) and first-principles theory (ii) is resolved by taking into account in the previous transport analysis the temperature dependence of the effective density of states, which leads to the result that the mobility is actually temperature-independent in Rh_2ZnO_4 . Our case study on Rh_2ZnO_4 illustrates the range of experimental and theoretical approaches at hand to determine whether the transport mechanism of a semiconductor is band or small polaron conduction.

I. Introduction

THE A_2BO_4 ^{††} oxide spinels have long been known and utilized for their soft magnetic/ferrimagnetic properties,¹ with more recent attention being given to their magnetoresistive² and multiferroic properties.³ Since the past decade, however, there has been increasing interest in their potential as transparent conductors^{4–6} with the possibility for applications in semiconductor devices and photovoltaics. For example, a p - n junction has been demonstrated using a p -type

spinel in the amorphous state.^{7,8} Determination of the mechanism of conductivity of holes in these potential transparent conducting oxides (TCOs) may be crucial for the future design of better p -type TCOs.

Electrical conductivity in spinel oxides is usually associated with materials that are wide-gap insulators in their stoichiometric and undoped perfect A_2BO_4 structure, but that become conductive owing to specific deviations from stoichiometry leading to generation of excess carriers. Examples of normal spinels that are wide gap insulators in their pristine A_2BO_4 form include systems where the trivalent A atom located on the octahedral site (O_h point group symmetry), as well as the divalent B atom located on the tetrahedral site (T_d), have a closed shell d^0 (e.g., Al, Mg) or d^{10} (e.g., Ga, Zn) configuration. In Rh_2ZnO_4 , where the Rh^{+III} ions have an open-shell d^6 configuration (low-spin, $S = 0$), the insulating gap is formed due to the crystal field splitting: After hybridizing with the O- p states, the fully occupied Rh- t_{2g} forms the valence band, and the unoccupied Rh- e_g state forms the conduction band, as shown in Fig. 1. Along the series of A_2ZnO_4 spinels ($A = \text{Co}, \text{Rh}, \text{Ir}$), the optical band gaps were measured as 2.26, 2.74, and 2.97 eV, respectively.⁴ A recent theoretical work by Scanlon *et al.*⁹ calls into question the magnitudes of these band gaps, but we note that these materials are at least partially transparent to lower energy visible light, making them candidate materials for p -type TCOs.

To obtain p -type conductivity in these otherwise insulating spinels, one must create acceptor-type lattice defects, which can result from off-stoichiometry at finite temperatures. As would-be hole producing cation vacancies require rather high energy to form,¹⁰ the main source of hole

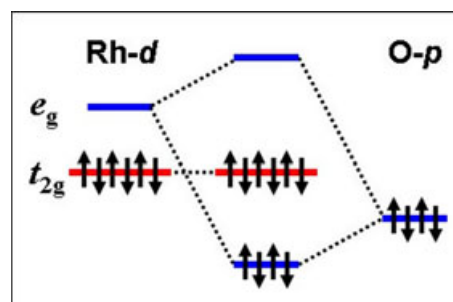


Fig. 1. Nature of the insulating gap in Rh_2ZnO_4 with a low-spin d^6 configuration of Rh^{+III} . On the O_h site, the atomic Rh- d orbitals split into e_g and t_{2g} crystal field states. The e_g orbitals interact with the O- p ligands forming an occupied bonding and an unoccupied anti-bonding state. Note that the HOMO t_{2g} orbitals are non-bonding.

W.-Y. Ching—contributing editor

Manuscript No. 29593. Received April 13, 2011; approved June 28, 2011.

This work was supported by the Basic Energy Science Division, U.S. Department of Energy, under Grant No. DE-AC36-08G028308 to NREL. The “Center for Inverse Design” is a DOE Energy Frontier Research Center. The high magnetic field work and use of the J. B. Cohen X-Ray Diffraction Facility were supported by the National Science Foundation’s MRSEC Program (DMR-0520513) at the Materials Research Center of Northwestern University.

*Member, The American Ceramic Society.

**Fellow, The American Ceramic Society.

[†]Author to whom correspondence should be addressed. e-mail: t-mason@northwestern.edu.

^{††}Another widely used way of writing the spinel chemical formula is AB_2O_4 . We, however, write A_2BO_4 , which is common for spinels with formal cation valencies $Z_A = 2$ and $Z_B = 4$ such as Mg_2TiO_4 . The main reason for our choice is the fact that the work presented here is part of a larger project that treats all A_2BX_4 compounds (not only spinels) in different structure-types including olivine Fe_2SiO_4 , β - K_2SO_4 or La_2CuO_4 for which A_2BX_4 is the generally used notation.

production in these spinels is the anti-site defect, where a B-cation substitutes for the A-cation on the O_h site, i.e., Zn_{Rh} in Rh_2ZnO_4 . In Rh_2ZnO_4 , at thermodynamic equilibrium, the calculated maximum number of acceptor-like anti-site defects $N(Zn_{Rh})$ is approximately 10^{20} cm^{-3} , whereas the number of cation vacancies $N(V_{Zn})$ is 10^{17} cm^{-3} and $N(V_{Rh})$ is 10^{14} cm^{-3} . The concentration of donor-like defects $N(Rh_{Zn})$ is 10^{15} cm^{-3} , and $N(V_O)$ is 10^{10} cm^{-3} . Spinel oxides in general can be divided into four “doping types (DTs)” depending upon the position of the main donor and acceptor levels with respect to the band edges. DT-I includes the usual materials in which the donor level lies above the acceptor level in the band gap, i.e., a material with both electrically active donors and acceptors. DT-II systems are *p*-type materials that have the acceptor level in the gap, and the donor level in the valence band continuum, i.e., a material with only an electrically active acceptor. DT-III would be *n*-type materials with the donor level in the gap and the acceptor level in the conduction band, i.e., a material with only an electrically active donor. DT-IV materials are insulators with deep donor levels below deep acceptor levels. A more thorough explanation of these doping types will be given in a separate work. Rh_2ZnO_4 has been found from first-principles calculations to be “doping Type II” and shows *p*-type behavior. Having identified the source of holes in non-stoichiometric spinels of the Rh_2ZnO_4 type, the next critical question is whether the conductivity is band-like with a potentially high mobility, or small polaron-like with a limited mobility.¹¹

It is well known^{12–15} that excess holes or excess electrons in polar materials could spatially localize around particular displaced crystal sites, leading to self-trapping (a “small polaron”) and impeded mobility.¹¹ The transport mechanism is referred to as small polaron hopping (SPH). However, the rules deciding if such self-trapped states are energetically favorable in a given system are still unclear. Theoretical predictions are based either on semi-quantitative model approaches (e.g., Mott-Littleton¹³), or on electronic structure calculations, which face the problem to either overly favor (Hartree-Fock methods) or disfavor (uncorrected density functional theory) polaronic localization.¹⁵ The experimental verification of small polaron conductivity, for example, in the transition metal monoxides, is often clouded by the effects of impurities and surfaces, and by temperature-dependent changes of the transport mechanism.^{14,16,17} A direct observation of free small polarons by electron spin resonance, measuring the hyperfine splitting, which serves as a microscopic fingerprint, was achieved in few cases,^{18,19} but in most ceramic studies, such data are not available. Yet, the understanding of whether excess carriers are lattice-bound or not is critical to future applications of materials such as *p*-type TCOs. In this article, we discuss the theoretical and experimental methodologies, applied to the transport mechanism for holes in Rh_2ZnO_4 establishing a procedure for deciding the type of conductivity in the absence of directly observable microscopic fingerprints.

In an earlier work, a thermally activated mobility has been interpreted to imply a small polaron mechanism, based on the activated mobility that was deduced from the temperature dependence of the conductivity and the Seebeck coefficient.⁵ However, without additional support, such commonly used interpretations based on temperature-dependent transport properties^{20–24} may lead to good fits to the data without rigorously implying a polaronic mechanism. Employing a recently developed *corrected* density functional first-principles theory, we find that self-trapping of holes is endothermic both at the Rh- and at the O-site, suggesting band, not polaronic conductivity. To gain further experimental clues about the transport mechanism, we performed high-field Hall-effect measurements (representing the first successful Hall measurement on Rh_2ZnO_4) from which we

determined a mobility of $\mu = 0.18 \text{ cm}^2/\text{Vs}$. This mobility lies above the Bosman & van Daal limit¹¹ for SPH ($\mu \ll 0.1 \text{ cm}^2/\text{Vs}$), hence suggesting that the mechanism is not small polaron transport. Finally, we re-examine the earlier transport analysis of Ref. [5], taking now into account that the effective density of states N_V is temperature-dependent, and find that in the corrected analysis, the mobility is not activated.

Taking into account the first-principles theory results, the high-field Hall-measurement and revised transport analysis, Rh_2ZnO_4 is consistently described as a band conductor. The relatively low mobility can be explained by the rather large effective density of states (see below), $N_V = 5 \times 10^{20} \text{ cm}^{-3}$ at 300 K, which corresponds to an effective mass of $m_h^* \approx 7 m_e$. This heavy hole mass originates from the fact that the highest occupied molecular orbital (HOMO) (Fig. 1) is a non-bonding state, and thus has no band-broadening due to Rh-*d*/O-*p* hybridization. Interestingly, a similar ambiguity concerning small polaron conduction has recently appeared in *p*-type CuAlO_2 ,^{22,25} where a small polaron mechanism was deduced for polycrystalline films,²² but band-conduction was observed in single crystals.²⁵ Such conflicts highlight the fact that temperature-dependent transport measurements by themselves are unable to unambiguously determine the type of the transport mechanism. Our present work illustrates the range of additional approaches available to conclusively answer the question whether band- or small polaron conductivity prevails. Furthermore, the agreement between theory and experiment opens the door to predicting the electronic properties of similar systems, facilitating an inverse approach to materials design.

II. Experimental Procedure

(1) Bulk Fabrication Methods

A bulk ceramic specimen of intentionally biphasic, Zn-rich Rh_2ZnO_4 was fabricated via solid-state reaction. Dry powders of rhodium (III) oxide (Strem Chemicals Inc., Newburyport, MA) with purity 99.9% and zinc oxide (Alfa Aesar, Ward Hill, MA) with purity 99.99% were weighed on a Mettler balance (Mettler-Toledo, Inc., Columbus, OH) with 0.1 mg accuracy and ground together thoroughly with mortar and pestle. A pellet approximately 12.5 mm in diameter and 1.5 mm in thickness was pressed at 125–130 MPa. The pellet was surrounded with sacrificial powder, placed in nested crucibles, fired at 975°C for 20 h, and slow-cooled in air at 5°/min to prevent cracking due to thermal shock. The sample was then re-ground and re-pressed, and subjected to the same heat treatment.

The phase content was confirmed via X-ray powder diffraction on a Rigaku diffractometer (Rigaku, The Woodlands, TX), with a $\text{CuK}\alpha$ radiation source and a Ni filter. A step size of 0.05° and a count time of 1 s were used. The X-ray pattern was matched to the *fd3m* (PDF: 41-0134) and $\text{P6}_3\text{mc}$ (PDF: 01-070-8072) space groups.

The sample was made intentionally biphasic because according to the Gibbs Phase Rule, at fixed temperature and pressure, the number of degrees of freedom in a thermodynamic system is $F = C - P$. In our three-component system, $F = 3 - P$, where P is the number of phases. If we set $P = 1$ (a single-phase system), then we must fix two variables at equilibrium: oxygen partial pressure, and η_{Zn}/η_{Rh} , the ratio of zinc to rhodium cations. Because of the sensitivity limits in measuring powders, this ratio is almost impossible to fix, leading to small variations in composition. However, if the number of phases is intentionally set to $P = 2$, then the only variable that must be fixed is the oxygen partial pressure, which is easily accomplished. We expect that the ZnO second phase is insulating and has a negligible effect on the conductivity of the sample. Electrical measurements on a sample of Rh-doped ZnO (95 mol% ZnO, 5 mol% Rh_2O_3) confirm insulating behavior.

(2) Transport Measurements

Room temperature four-point DC conductivity and thermo-power measurements were taken. The specimen was then cut into a bar-shaped geometry with dimensions approximately $10.5 \text{ mm} \times 4.5 \text{ mm} \times 1.5 \text{ mm}$, and *in-situ* electrical measurements were performed from 250°C to 580°C using a previously reported technique.^{26,27} For the Hall measurement, the sample was attached to the copper tongue of an 8-pin mount by a thin layer of adhesive grease, which was thermally conductive, but electrically insulating. Four silver stripes were pasted to the four sides of the sample, the width ranging from 1.7 to 3.0 mm, and four indium contacts were soldered onto the stripes. The indium contacts could not be directly soldered to the sample because of its relatively high thermal conductivity. The Van der Pauw method was used to measure Hall resistivity as a function of magnetic field. As the widths of the silver stripes (and hence the effective contact areas) were large compared with the sample dimensions, the Hall measurement was accurate to within 20%. Hall measurements were carried out in a magnetic field up to 15 T with a 1.7 Hz alternating current source using lock-in techniques, and averaging four up-and-down magnetic field sweeps of both polarities. The data between 0 and 1 T have been removed as they represent purely instrumental noise.

III. Results and Discussion

(1) Predictive First-Principles Theory for the Nature of Holes in Rh_2ZnO_4

To predict from electronic structure theory whether a semiconductor (or insulator) shows band- or small polaron conductivity, one needs a method that accurately describes the energy difference between the delocalized state at the band edge (here, the valence band maximum), and the localized self-trapped state, which can usually be described by a change in the oxidation state (here, Rh^{+IV} instead of Rh^{+III} or O^{-I} instead of O^{-II}). Unfortunately, this requirement is not generally fulfilled by standard electronic structure methods, like local density or Hartree-Fock calculations. The key to recover the correct energy difference is to satisfy the generalized Koopmans condition,²⁸

$$E(N+1) - E(N) = e_{N+1}(N) \quad (1)$$

requiring that the $N \rightarrow N+1$ electron addition energy E_{add} equals the single-particle energy e_{N+1} of the unoccupied self-trapped hole state in the N electron system before electron addition. To predict the binding energies of acceptor states that have the characteristic of impurity bound small polarons,²⁹ we have introduced in Ref. [28] a ‘‘hole-state potential’’ V_{hs} , whose strength is controlled by a parameter λ_{hs} , which can be varied to satisfy the condition in Eq. (1). The value of the parameter λ_{hs} is not empirically adjusted, but instead, it is determined so to satisfy the physical condition in Eq. (1).

The potential V_{hs} is added to a standard density functional calculation using the projector-augmented wave method implemented in the VASP code.³⁰ We use the exchange correlation functional of Ref. [31] and the DFT+U method of Ref. [32] (the moderate Coulomb energy of $U = 3 \text{ eV}$, used for the Rh-*d* and Ti-*d* orbitals, yields generally improved band-structure and thermochemical properties in transition metal oxides³³). Finite-size effects in charged supercells have been corrected for both the total³⁴ and the single-particle³⁵ energies in Eq. (1). Convergence tests have been performed for the energy cutoff, Brillouin zone sampling and supercell size, using cells up to 216 atoms.

We now apply the polaron theory, initially developed for and applied to defect bound polarons,²⁸ to the case of free hole carriers, which allows us to predict theoretically the conduction type (band-like or small polaron). We show in

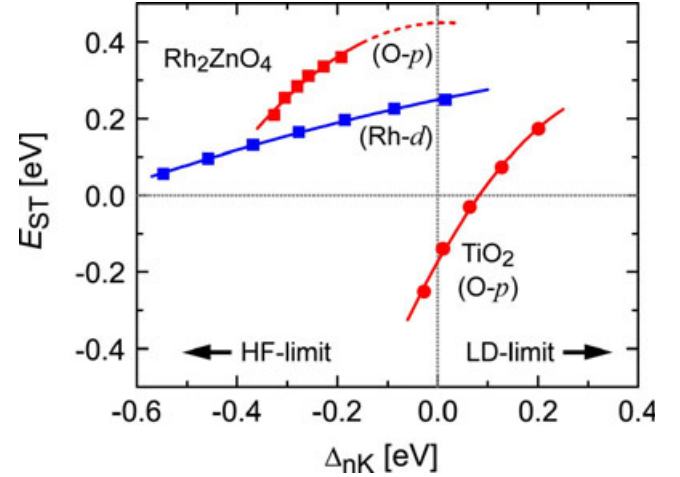


Fig. 2. The polaron self-trapping energy E_{ST} as a function of the non-Koopmans energy Δ_{nK} for the Rh-*d* and O-*p* holes in Rh_2ZnO_4 (squares) and for the O-*p* hole in TiO_2 (circles). At the physically correct condition $\Delta_{\text{nK}} = 0$, the self-trapping is endothermic in Rh_2ZnO_4 , but exothermic in TiO_2 . The arrows indicate the trends of Hartree-Fock (HF) and local density (LD) calculations, which do not satisfy $\Delta_{\text{nK}} = 0$.

Fig. 2 the hole self-trapping (ST) energy $E_{\text{ST}} = E_{\text{SP}} - E_{\text{VB}}$ as a function of the non-Koopmans energy $\Delta_{\text{nK}} = E_{\text{add}} - e_{N+1}$. Here, E_{SP} and E_{VB} are the total energies for the hole in the localized small-polaron (SP) and in the delocalized valence-band (VB) states, respectively.

We see in Fig. 2 that the self-trapping energy in Rh_2ZnO_4 is positive (endothermic) for both the Rh-*d* and O-*p* holes (Rh^{+IV} and O^{-I} , respectively). The *polaronic* Rh-*d* hole exists as a metastable state with a local minimum 0.25 eV above the ground-state delocalized valence band state. The O-*p* hole is obtained in the calculation as a local minimum only for excessively large parameters λ_{hs} , but decays spontaneously into the band-like state for a value of λ_{hs} at which the Koopmans condition, Eq. (1) is fulfilled. From extrapolation (see Fig. 2), we estimate $E_{\text{ST}} = +0.4 \text{ eV}$ for the O-*p* hole in Rh_2ZnO_4 . Thus, our first-principles theory for a polaronic hole state predicts Rh_2ZnO_4 as a band conductor. When we apply the same methodology to the O-*p* hole in rutile TiO_2 , where the formation of a small hole polaron in TiO_2 has been inferred from electron spin resonance,¹⁹ we find indeed an exothermic self-trapping energy $E_{\text{ST}} = -0.18 \text{ eV}$.

To understand why, according to theory, small polarons are unstable in Rh_2ZnO_4 , we recall that the self-trapping energy can be written as the sum of a localization energy and a relaxation energy,³⁶

$$E_{\text{ST}} = E_{\text{loc}} - E_{\text{rel}} \quad (2)$$

Thus, an exothermic E_{ST} requires that the relaxation energy exceeds the localization energy. As seen in Fig. 1, the valence band maximum (i.e., the HOMO) of Rh_2ZnO_4 is formed predominantly by the non-bonding t_{2g} crystal field state of the Rh-*d* orbitals. In the O_h point group symmetry of the A site in the spinel lattice, this non-bonding state does not interact with the *p*-orbitals of the O ligands. Therefore, a trapping of a hole in the Rh- t_{2g} state does not lead to the breaking of a bond, which would cause large relaxations. Thus, the small relaxation energy is not sufficient to stabilize the small polaron. In contrast, the self-trapping of an O-*p* hole breaks one of the bonds that is formed between the Rh- e_g state and the O-*p* ligands (see Fig. 1), leading to a large relaxation energy in the order of 1 eV. However, as the O-*p* orbitals lie at energies below the Rh- t_{2g} state that forms the upper valence band (see Fig. 1), there is a large energy cost E_{loc} to

localize a hole in an O-*p* orbital at such energies far below the VBM. In the sum, $E_{\text{loc}} - E_{\text{rel}}$ remains positive (see Fig. 2).

We conclude that employing the recently developed corrected density functional first-principles theory we find that self-trapping of holes is endothermic both at the Rh- and at the O-site, suggesting band, not polaronic conductivity.

(2) High-Field Hall-Effect Measurements

From the analysis of conductivity and thermopower measurements in Ref. [5], the room temperature mobility of Rh_2ZnO_4 was estimated as $2.8 \times 10^{-4} \text{ cm}^2/\text{Vs}$. For such low values, traditional Hall effect measurements are extremely challenging, making direct measurement of the carrier density a difficult task. Yet, it is precisely this type of measurement that can provide rather strong evidence for conductivity type in the absence of a direct microscopic measurement of free small polarons by electron spin resonance.^{18,19}

Here, we use a high-field setup allowing the measurement of the Hall effect up to 15 T. We synthesized a bulk, polycrystalline sample of nominally 90 mol% Rh_2ZnO_4 and 10 mol% ZnO prepared as described above. For these conditions, which lead to the creation of an excess of Zn_{Rh} antisite acceptors, we predict a net acceptor concentration of $N_{\text{A}} - N_{\text{D}} \approx 10^{20} \text{ cm}^{-3}$ from our defect formation energy calculations and thermodynamic modeling.¹⁰ As shown in Fig. 3, we report here the first successful Hall measurement on Rh_2ZnO_4 , in either bulk or thin film form. The resulting hole density of $1.4 \pm 0.3 \times 10^{20} \text{ cm}^{-3}$ is consistent with the predicted net acceptor concentration.

The room temperature conductivity was measured to be 0.84 S/cm by the four-point method. However, because this sample is a bulk, porous, polycrystalline specimen, the conductivity is corrected for porosity by employing the method outlined by McLachlan *et al.*²⁶ In this calculation, the conductivity of the conducting phase is given by

$$\sigma_{\text{h}} = \frac{\sigma_{\text{m}}}{1 - \frac{3}{2}f} \quad (3)$$

where σ_{m} is the conductivity of the composite, and f is the porosity fraction of the sample. The sample density was determined by measuring the dimensions and mass of the pellet. The resulting calculated density of 3.416 g/cm^3 was then divided by the theoretical density of 7.225 g/cm^3 to obtain a density fraction of 0.47, or a value of 0.53 for f .

Using this corrected conductivity of 4.0 S/cm, we obtain a mobility of $0.18 \text{ cm}^2/\text{Vs}$, which is much larger than the previ-

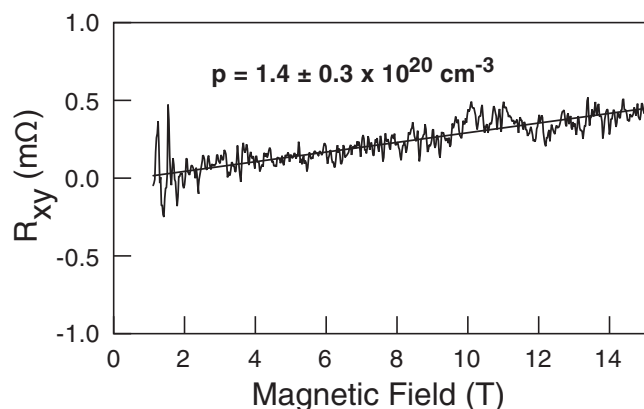


Fig. 3. The Hall resistance R_{xy} in a high-field setup, as a function of the magnetic field, yielding a hole density of $p = 1.4 \pm 0.3 \times 10^{20} \text{ cm}^{-3}$. The data between 0 and 1 T have been removed as they represent purely instrumental noise.

ous estimate in Ref. [5], and also lies above the theoretical limit, $\mu \ll 0.1 \text{ cm}^2/\text{Vs}$, for SPH as described by Bosman and van Daal.¹¹ This mobility value should be considered a lower limit, given the polycrystalline nature of the bulk specimen employed. For example, bulk polycrystalline specimens of the p-type TCO, CuAlO_2 , exhibited similar room temperature mobilities on the order of $0.1 \text{ cm}^2/\text{Vs}$ or less.^{22,37} However, single crystal values proved to be much higher ($3 \text{ cm}^2/\text{Vs}$ in the a-b plane).²⁵

The high-field Hall measurements support the picture of band conductivity, which we obtained by theory in the previous section. Although Hall effect versus temperature would provide additional evidence for the non-activated mobility, the apparatus employed was incapable of measurements in the high temperature range of the electrical conductivity and Seebeck coefficient measurements (250°C – 580°C).

(3) Re-Examination of the Transport Analysis

Figure 4(a) shows high temperature simultaneous four point conductivity and thermopower measurements from $T = 250^\circ\text{C}$ to 580°C . Over this temperature range, the conductivity changes significantly, but the thermopower is relatively constant, only varying by about $20 \mu\text{V/K}$. Traditionally, this behavior has been interpreted to be characteristic of an activated mobility. The latter was often assumed to reflect polaronic conductance. We repeat the main steps of the traditional analysis to disclose some subtle points.

The expressions for conductivity ($\sigma = pe\mu$) and reduced thermopower,

$$Q_{\text{red}} = -\frac{Q}{k/e} = (\ln p - \ln N_{\text{V}} - A) \quad (4)$$

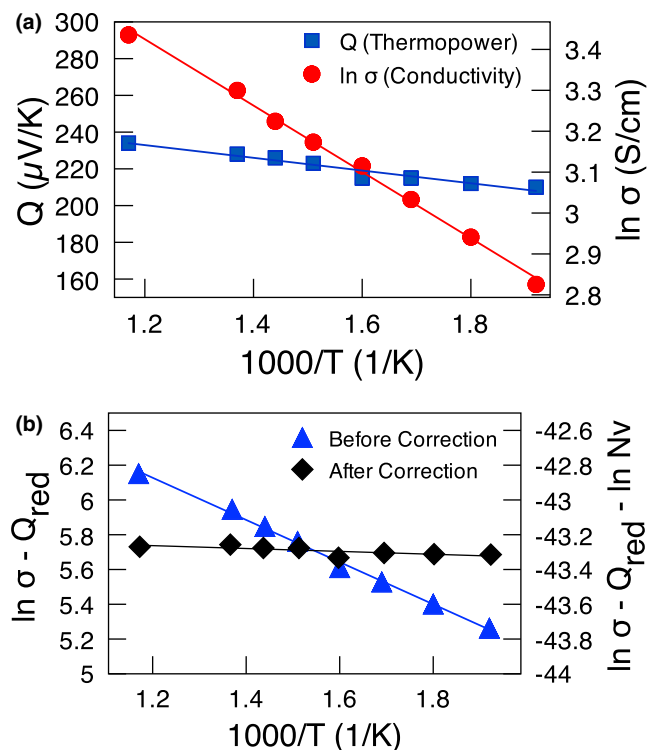


Fig. 4. (a) Conductivity and thermopower data from $T = 250^\circ\text{C}$ to 580°C . The conductivity changes significantly, but the thermopower remains relatively constant. (b) Activated mobility analysis before and after the correction for the temperature dependence of the effective density of states $N_{\text{V}}(T)$ is considered. After the correction, a slope of nearly zero is obtained, indicating that the mobility is not activated. The ordinate axis on both plots spans the same range.

can be combined to eliminate the carrier density p :

$$\ln \sigma - Q_{\text{red}} = \ln \mu + \ln N_V + \ln e + A \quad (5)$$

Here, μ is the mobility, e is the elementary charge, k is the Boltzmann constant, N_V is the so-called effective density of states, and A is a transport constant (between 2 and 4 for band conduction, and typically zero for SPH^{24,38}). The mobility in a small polaron system is described by

$$\mu = \frac{g(1-c)ea^2v}{kT} \exp\left(\frac{-E_H}{kT}\right) \quad (6)$$

where g is a geometric factor, a is the jump distance between hopping sites, $1-c$ is the probability that a neighboring site is available for exchange, v is the phonon frequency, and E_H is the hopping activation energy. In the traditional polaron analysis, the experimental data are plotted as $\ln \sigma - Q_{\text{red}}$ vs $1/T$. Assuming that the effective density of states is independent of temperature, the slope of this plot yields the temperature dependence of the mobility, as shown in Eq. (7)

$$\frac{\partial(\ln \sigma - Q_{\text{red}})}{\partial(1/T)} = \frac{\partial(\ln \mu)}{\partial(1/T)} \quad (7)$$

By applying the small polaron analysis from Ref. [5], “reasonable values” for the hopping energy ($E_H = 0.16$ eV) and the phonon frequency ($v = 4.25 \times 10^{13}$ Hz) are obtained. In the past, this self-consistent analysis alone was enough to conclude small polaron hopping.

It turns out that the backing out from such a fit a reasonable positive value of E_H (i.e., bound polaron behavior) does not provide a stringent demand on the data fitting. Indeed, if we explicitly evaluate a temperature-dependent effective density of states $N_V(T)$ from the (density-functional) calculated density of states $g(E)$ of Rh_2ZnO_4 ,

$$N_V(T) = \int_{-\infty}^{E_{\text{VBM}}} g(E) \exp^{-(E_{\text{VBM}}-E)/kT} dE \quad (8)$$

and plot $\ln \sigma - Q_{\text{red}} - \ln N_V$ vs $1/T$, we see in Fig. 4(b) that the mobility is practically constant when this temperature dependence is taken into account. In the absence of an activated mobility, Rh_2ZnO_4 must be a band conductor, and not a small polaron conductor. For a sensible value $A = 2$, we obtain a mobility $\mu = 0.12$ cm²/Vs, demonstrating that the revised high-temperature transport analysis is consistent with the picture obtained from the room temperature Hall measurement (see above).

IV. Conclusion

By incorporating recent methods in correcting density functional theory methodologies for hole localization, we have shown that theory predicts Rh_2ZnO_4 to be a band conductor. In contrast, the high temperature electrical properties of a bulk ceramic specimen were measured and traditional analysis shows that the system has an activated mobility, which is usually interpreted as an indication of small polaron conduction. However, by incorporating the temperature dependence of the effective density of states into our analysis, we have shown that the mobility is independent of temperature. A room temperature Hall effect measurement on this sample confirms that the mobility in this system is much higher than previously thought, consistent with band conduction. These findings indicate that the fundamental limitation in some spinel oxides is a heavy hole mass, instead of a

self-trapping hole, opening the door to the possibility of discovering a transparent conductor with a light hole mass through first principles.

References

- ¹S. Krupicka and P. Novak, “Oxide Spinel”; pp. 191–210 in *Handbook of Ferromagnetic Materials*, Vol. 3. Edited by E. P. Wohlfarth. North-Holland Physics Publishing, Amsterdam, 1982.
- ²J. Philip and T. R. N. Kutty, “Colossal Magnetoresistance of Oxide Spinels, $\text{Co}_x\text{Mn}_{3-x}\text{O}_4$,” *Mater. Lett.*, **39** [6] 311–7 (1999).
- ³Y. Yamasaki, S. Miyasaka, Y. Kaneko, J. P. He, T. Arima, and Y. Tokura, “Magnetic Reversal of the Ferroelectric Polarization in a Multiferroic Spinel Oxide,” *Phys. Rev. Lett.*, **96** [20] 207204 (2006).
- ⁴M. Dekkers, G. Rijnders, and D. H. A. Blank, “ ZnIr_2O_4 , a p-Type Transparent Oxide Semiconductor in the Class of Spinel Zinc-d(6)-Transition Metal Oxide,” *Appl. Phys. Lett.*, **90** [2] 021903 (2007).
- ⁵N. Mansourian-Hadavi, S. Wansom, N. H. Perry, A. R. Nagaraja, T. O. Mason, L. H. Ye, and A. J. Freeman, “Transport and Band Structure Studies of Crystalline ZnRh_2O_4 ,” *Phys. Rev. B*, **81** [7] 075112 (2010).
- ⁶H. Mizoguchi, M. Hirano, S. Fujitsu, T. Takeuchi, K. Ueda, and H. Hosono, “ ZnRh_2O_4 : A p-Type Semiconducting Oxide with a Valence Band Composed of a Low Spin State of Rh^{3+} in a 4d(6) Configuration,” *Appl. Phys. Lett.*, **80** [7] 1207–9 (2002).
- ⁷T. Kamiya, S. Narushima, H. Mizoguchi, K. Shimizu, K. Ueda, H. Ohta, M. Hirano, and H. Hosono, “Electrical Properties and Structure of p-Type Amorphous Oxide Semiconductor $\text{XZnO} \cdot \text{Rh}_2\text{O}_3$,” *Adv. Funct. Mater.*, **15** [6] 968–74 (2005).
- ⁸S. Narushima, H. Mizoguchi, K. Shimizu, K. Ueda, H. Ohta, M. Hirano, T. Kamiya, and H. Hosono, “A p-Type Amorphous Oxide Semiconductor and Room Temperature Fabrication of Amorphous Oxide p-n Heterojunction Diodes,” *Adv. Mater.*, **15** [17] 1409–13 (2003).
- ⁹D. O. Scanlon and G. W. Watson, “Band gap Anomalies of the (ZnM_2O_4) -O-III (M-III = Co, Rh, Ir) Spinels,” *Phys. Chem. Chem. Phys.*, **13** [20] 9667–75 (2011).
- ¹⁰T. R. Paudel, S. Lany, M. d’Avezac, A. Zunger, N. H. Perry, A. R. Nagaraja, T. O. Mason, J. S. Bettinger, Y. Shi, and M. F. Toney, “Asymmetric Cation Non-Stoichiometry in Spinels: Site Occupancy in Co_2ZnO_4 and Rh_2ZnO_4 ,” *Phys. Rev. B* (in press), doi: 10.1103/PhysRevB.00.00410.
- ¹¹A. J. Bosman and H. J. van Daal, “Small-Polaron Versus Band Conduction in Some Transition-Metal Oxides,” *Adv. Phys.*, **19** [77] 1–117 (1970).
- ¹²D. Emin, “Small Polarons,” *Phys. Today*, **35** [6] 34–40 (1982).
- ¹³N. F. Mott and M. J. Littleton, “Conduction in Polar Crystals, Electrolytic Conduction in Solid Salts (Reprinted From, Vol 34, Pg 485, 1938),” *J. Chem. Soc. - Faraday Trans.*, **85**, 565–79 (1989).
- ¹⁴A. M. Stoneham, “Small Polarons and Polaron Transitions,” *J. Chem. Soc. - Faraday Trans.*, **85**, 505–16 (1989).
- ¹⁵A. M. Stoneham, J. Gavartin, A. L. Shluger, A. V. Kimmel, D. M. Ramo, H. M. Ronnow, G. Aeppli, and C. Renner, “Trapping, Self-Trapping and the Polaron Family,” *J. Phys. Condens. Matter.*, **19** [25] 255208 (2007).
- ¹⁶D. P. Dobson, N. C. Richmond, and J. P. Brodholt, “A High-Temperature Electrical Conduction Mechanism in the Lower Mantle Phase $(\text{Mg,Fe})\text{O}_{(1-x)}$,” *Science*, **275** [5307] 1779–81 (1997).
- ¹⁷E. Gartstein and T. O. Mason, “Reanalysis of Wustite Electrical Properties,” *J. Am. Ceram. Soc.*, **65** [2] C24–6 (1982).
- ¹⁸O. F. Schirmer and E. Salje, “Conduction Bipolarons in Low-Temperature Crystalline $\text{WO}_{(3-x)}$,” *J. Phys. C Solid State*, **13** [36] 1067–72 (1980).
- ¹⁹S. Yang, L. E. Halliburton, A. Manivannan, P. H. Bunton, D. B. Baker, M. Klemm, S. Horn, and A. Fujishima, “Photoinduced Electron Paramagnetic Resonance Study of Electron Traps in TiO_2 Crystals: Oxygen Vacancies and Ti^{3+} Ions,” *Appl. Phys. Lett.*, **94** [16] 162114 (2009).
- ²⁰E. Asenath-Smith, I. N. Lokuhepa, S. T. Misture, and D. D. Edwards, “p-Type Thermoelectric Properties of the Oxygen-Deficient Perovskite $\text{Ca}_2\text{Fe}_2\text{O}_5$ in the Brownillerite Structure,” *J. Solid State Chem.*, **183** [7] 1670–7 (2010).
- ²¹H. C. Chen, E. Gartstein, and T. O. Mason, “Conduction Mechanism Analysis for $\text{Fe}_{(1-\delta)}\text{O}$ and $\text{Co}_{(1-\delta)}\text{O}$,” *J. Phys. Chem. Solids*, **43** [10] 991–5 (1982).
- ²²B. J. Ingram, T. O. Mason, R. Asahi, K. T. Park, and A. J. Freeman, “Electronic Structure and Small Polaron Hole Transport of Copper Aluminate,” *Phys. Rev. B*, **64** [15] 155114 (2001).
- ²³D. P. Karim and A. T. Aldred, “Localized Level Hopping Transport in $\text{La}(\text{Sr})\text{CrO}_3$,” *Phys. Rev. B*, **20** [6] 2255–63 (1979).
- ²⁴H. L. Tuller and A. S. Nowick, “Small Polaron Electron-Transport in Reduced CeO_2 Single-Crystals,” *J. Phys. Chem. Solids*, **38** [8] 859–67 (1977).
- ²⁵J. Tate, H. L. Ju, J. C. Moon, A. Zakutayev, A. P. Richard, J. Russell, and D. H. McIntyre, “Origin of p-Type Conduction in Single-Crystal CuAlO_2 ,” *Phys. Rev. B*, **80** [16] 165206 (2009).
- ²⁶D. S. McLachlan, M. Blaszkiewicz, and R. E. Newnham, “Electrical-Resistivity of Composites,” *J. Am. Ceram. Soc.*, **73** [8] 2187–203 (1990).
- ²⁷A. Trestman-Matts, S. E. Dorris, and T. O. Mason, “Measurement and Interpretation of Thermopower in Oxides,” *J. Am. Ceram. Soc.*, **66** [8] 589–92 (1983).
- ²⁸S. Lany and A. Zunger, “Polaronic Hole Localization and Multiple Hole Binding of Acceptors in Oxide Wide-Gap Semiconductors,” *Phys. Rev. B*, **80** [8] 085202 (2009).

²⁹O. F. Schirmer, "O⁻ Bound Small Polarons in Oxide Materials," *J. Phys. Condens. Matter.*, **18** [43] R667–704 (2006).

³⁰G. Kresse and D. Joubert, "From Ultrasoft Pseudopotentials to the Projector Augmented-Wave Method," *Phys. Rev. B*, **59** [3] 1758–75 (1999).

³¹J. P. Perdew, K. Burke, and M. Ernzerhof, "Generalized Gradient Approximation Made Simple," *Phys. Rev. Lett.*, **77** [18] 3865–8 (1996).

³²S. L. Dudarev, G. A. Botton, S. Y. Savrasov, C. J. Humphreys, and A. P. Sutton, "Electron-Energy-Loss Spectra and the Structural Stability of Nickel Oxide: An LSDA+U Study," *Phys. Rev. B*, **57** [3] 1505–9 (1998).

³³S. Lany, J. Osorio-Guillén, and A. Zunger, "Origins of the Doping Asymmetry in Oxides: Hole Doping in NiO Versus Electron Doping in ZnO," *Phys. Rev. B*, **75** [24] 241203(R) (2007).

³⁴S. Lany and A. Zunger, "Assessment of Correction Methods for the Band-Gap Problem and for Finite-Size Effects in Supercell Defect Calculations: Case Studies for ZnO and GaAs," *Phys. Rev. B*, **78** [23] 235104 (2008).

³⁵S. Lany and A. Zunger, "Many-Body GW Calculation of the Oxygen Vacancy in ZnO," *Phys. Rev. B*, **81** [11] 113201 (2010).

³⁶E. N. Heifets and A. L. Shluger, "The Calculation of the Self-Trapping Energy in Crystals with Mixed-Valence Band," *J. Phys. Condens. Matter.*, **4** [43] 8311–20 (1992).

³⁷F. A. Benko and F. P. Koffyberg, "Opto-Electronic Properties of CuAlO₂," *J. Phys. Chem. Solids*, **45** [1] 57–9 (1984).

³⁸A. F. Ioffe, *Physics of Semiconductors. (Translated from Russian)*, Information, London, 1960. □